

## Simulation of greenhouse energy and strawberry (*Seolhyang* sp.) yield using TRNSYS DVBES: A base case



Qazeem Opeyemi Ogunlowo<sup>a,b</sup>, Timothy Denen Akpenpuun<sup>c,d</sup>, Wook Ho Na<sup>c</sup>, Misbaudeen Aderemi Adesanya<sup>a</sup>, Anis Rabiu<sup>a</sup>, Prabhat Dutta<sup>e</sup>, Hyeon-Tae Kim<sup>f</sup>, Hyun-Woo Lee<sup>a,c,\*</sup>

<sup>a</sup> Department of Agricultural Civil Engineering, College of Agriculture and Life Sciences, Kyungpook National University, Daegu 702-701, Korea

<sup>b</sup> Department of Agricultural and Bioenvironmental Engineering, Federal College of Agriculture Ibadan, PMB 5029, Ibadan, Nigeria

<sup>c</sup> Smart Agriculture Innovation Center, Kyungpook National University, Daegu 41566, Korea

<sup>d</sup> Department of Agricultural and Biosystems Engineering, University of Ilorin, PMB 1515, Ilorin 240003, Nigeria

<sup>e</sup> Department of Food Security and Agricultural Development, Kyungpook National University, Daegu 702-701, Korea

<sup>f</sup> Department of Bio-Industrial Machinery, Gyeongsang National University, Jinju 52828, Korea

### ARTICLE INFO

#### Keywords:

Base case  
Energy demand  
DVBES  
Strawberry  
Yield  
TRNSYS 18

### ABSTRACT

This research establishes a base case scenario encompassing the energy behavior of the greenhouse and its direct influence on the yield of strawberries (*Seolhyang* sp.) to evaluate the performance of the greenhouse energy demand and its effect on crop yield. The objective is to develop a ventilated discretized volume building energy simulation (DVBES) that predicts energy demand, temperature, and relative humidity (RH) of a greenhouse and develop a predictive strawberry yield model that predicts the strawberry yield. This study used two single-span double-layer experimental greenhouses with different features. Experimentation was conducted in the winter season of 2021–2022 and 2022–2023. Hourly temperature, RH, and daily fuel consumption were used to validate the DVBES model. Weekly temperature, RH, solar radiation (SR), and yield were used to validate the strawberry yield model. The results show high prediction accuracy with minor errors. For a single-span double-layer greenhouse at E–W (90°) orientation, the total energy demand and strawberry yield were  $113.861 \text{ MJ.m}^{-2}$  and  $0.466 \text{ kg.plant}^{-1}.\text{season}^{-1}$ , respectively. The findings serve as a foundation for further research on optimizing energy consumption in greenhouse environments. This research contributes to advancing knowledge in sustainable agriculture and facilitates the transition toward a greener and more resource-conscious future.

### 1. Introduction

Strawberries are a popular fruit that is grown in greenhouses worldwide. Greenhouses provide a controlled environment, allowing strawberries to be grown year-round, regardless of the outside weather. However, they also require significant energy to heat and cool, which can be a major expense for greenhouse growers. Several ways exist to reduce the energy consumption of greenhouses. These include the use of energy-efficient greenhouse technologies and the use of computer simulations to optimize the greenhouse environment.

Computer simulations can predict greenhouses' energy consumption and identify ways to improve energy efficiency through building energy

simulation (BES.) Computational fluid dynamics (CFD), EnergyPlus, and TRNSYS are common BES tools. BES is a method for predicting and analyzing instantaneous energy demand based on several dynamic simulation techniques [1]. An artificial greenhouse-building A BES model can be created to take in weather information, material parameters for the envelope, and energy production.

While Mazzeo et al. [2] developed a BES model to assess the prediction accuracy of building performance simulation (BPS) tools, namely TRNSYS, EnergyPlus, and IDA ICE, and successfully validated their model with experimental measurements, Rasheed et al. [3] developed and validated a BES model to investigate the effect of various thermal screens, natural ventilation, and heating setpoint controls on annual and maximum heating loads of a multi-span greenhouse.

\* Corresponding author.

E-mail addresses: [ogunlowoqazeem@knu.ac.kr](mailto:ogunlowoqazeem@knu.ac.kr) (Q. Opeyemi Ogunlowo), [akpenpuun.td@unilorin.edu.ng](mailto:akpenpuun.td@unilorin.edu.ng) (T. Denen Akpenpuun), [wooks121@knu.ac.kr](mailto:wooks121@knu.ac.kr) (W. Ho Na), [misbauadesanya@knu.ac.kr](mailto:misbauadesanya@knu.ac.kr) (M. Aderemi Adesanya), [rabiuanis@knu.ac.kr](mailto:rabiuanis@knu.ac.kr) (A. Rabiu), [prabhat2035@knu.ac.kr](mailto:prabhat2035@knu.ac.kr) (P. Dutta), [bioani@gnu.ac.kr](mailto:bioani@gnu.ac.kr) (H.-T. Kim), [whlee@knu.ac.kr](mailto:whlee@knu.ac.kr) (H.-W. Lee).

<b>Nomenclature</b>		
$A_{sub}$	Substrate area ( $\text{m}^2$ )	
$Av$	Mean of the experimental data points	
$c$	Specific heat capacity of PCM ( $\text{kJ/kg K}$ )	
$c_{air}$	Air density ( $\text{kg/m}^3$ )	
$c_s$	Specific heat capacity of PCM at solid-state ( $\text{kJ/kg K}$ )	
$c_l$	Specific heat capacity of PCM at liquid state ( $\text{kJ/kg K}$ )	
$c_c$	Specific heat capacity of container ( $\text{kJ/kg K}$ )	
$c_v$	Specific heat capacity of the vapour ( $\text{J/(kg K)}$ )	
$e_a$	Average hourly actual vapour pressure (kPa)	
$e_o$	Saturation vapour pressure at air temperature $T_{hr}$ (kPa)	
$ET_o$	Evapotranspiration (mm/h)	
$Exp_i$	Experimental value	
$G$	Soil heat flux density ( $\text{MJ/m}^2 \text{ h}$ )	
$L$	Latent heat of PCM ( $\text{kJ/kg}$ )	
$LAI$	Leaf area index ( $\text{m}^2 \cdot \text{m}^{-2}$ )	
$m$	Mass of the PCM (kg)	
$m_{ETO}$	Evapotranspiration mass flow (kg/h)	
$N$	Data population	
$\dot{q}$	Energy rate (gain or loss) (kJ/hr)	
$Q_{air}$	Change of internal energy of zone calculated with capacitance of air (kJ/hr)	
$Q_{coup}$	Coupling gains (kJ/hr)	
$Q_{crop}$	Crop gain due to temperature difference between crop and its environment (kJ/hr)	
$Q_{cropT}$	Total crop gains (kJ/hr)	
$Q_{D\_Demand}$	Total energy demand (kJ/hr)	
$Q_{ET}$	Crop gain due to evapotranspiration (kJ/hr)	
$Q_{int}$	Internal gains (kJ/hr)	
$Q_{inf}$	Infiltration gains (kJ/hr)	
$Q_{pcm}$	PCM gains (kJ/hr)	
$Q_{sol}$	Absorbed solar gains on all inside surfaces of zones (kJ/hr)	
$Q_{solair}$	Convective energy gain of zone due to the transmitted SR through external windows which is transformed immediately into a convective heat flow to internal air (kJ/hr)	
$Q_{trans}$	Transmission into the surface from the inner surface node (kJ/hr)	
$Q_{vent}$	Ventilation gains (kJ/hr)	
$Q_{wgain}$	Wall gains (kJ/hr)	
$u_2$	Average hourly wind speed (m/s)	
$V$	Volume of PCM ( $\text{m}^3$ )	
$V_s$	Volume of PCM at solid-state ( $\text{m}^3$ )	
$V_p$	Volume of PCM at phase state ( $\text{m}^3$ )	
$V_l$	Volume of PCM in liquid form ( $\text{m}^3$ )	
$V_c$	Volume of container ( $\text{m}^3$ )	
<i>Greek symbols</i>		
$\rho$	Air density ( $\text{kg/m}^3$ )	
$\rho_s$	Density of PCM ( $\text{kg/m}^3$ )	
$\rho_p$	Density of PCM at solid-state ( $\text{kg/m}^3$ )	
$\rho_l$	Density of PCM at phase state ( $\text{kg/m}^3$ )	
$\rho_c$	Density of PCM at liquid state ( $\text{kg/m}^3$ )	
$\emptyset$	Density of container ( $\text{kg/m}^3$ )	
$\Delta T$	Pipe diameter (m)	
$\Delta$	Saturation slope vapour pressure curve at $T_{hr}$ (kPa/ $^\circ\text{C}$ )	
$\gamma$	psychrometric constant (kPa/ $^\circ\text{C}$ )	
<i>Abbreviations</i>		
Adj	Adjacent	
BF	Bench frames	
CVRMSE	Coefficient of variance of the root mean squared error	
DVBES	Discretized volume building energy simulation	
Ext	External	
FLF	First layer frame	
MW	Mineral wool	
NMBE	Normalized mean bias error	
PAR	Photosynthetic active radiation	
PO	Polyolefin	
QGH	Q greenhouse	
RGH	R greenhouse	
RH	Relative humidity	
RMSE	Root mean squared error	
SR	Solar reflectance	
ST	Solar transmittance	
T	Thickness	
TC	Thermal conductivity	
TRE	Thermal radiation emission	
TRNSYS	Transient system simulation	
TRNBuild	TRNSYS building model	
TRT	Thermal radiation transmittance	
TS	Thermal screen	
VRR	Visible radiation reflectance	
VRT	Visible radiation transmittance	

Contrarily, Boulard, et al. [4] and Asa'd et al. [5] created BES models that, using the idea of a porous medium, successfully simulated the dynamic influence of insect screens and tomato crops on airflow movement and, respectively, investigated the effectiveness of a rock-bed thermal storage heating system of an attached solar greenhouse. Because it enables the introduction of new models that may be linked together, TRNSYS is noted for its flexibility in contrast to CFD and EnergyPlus; this is why it is so widely used.

Researchers like Adesanya et al., Choab et al., Rabiu et al., Rasheed et al. (a), and Ward et al., [6–11] used TRNSYS to successfully model the greenhouse energy demand by comparing the mean indoor and ambient temperatures. Even though numerous places in experimental greenhouses were used to collect data, only one thermal point or node was considered in the building simulation. Despite the installation of distribution fans, studies by Cesar et al. [12], Lamrani et al. [13], and Zhao et al. [14] have shown that there is significant variation in the distribution of greenhouse microclimate parameters such as temperature, RH, SR, CO<sub>2</sub>, and VPD along the vertical axis and horizontal dimensions in greenhouses [15]. Baglivo et al. [16] claim that this variation causes

thermal stratification, which impacts the control of natural ventilation, and shows that volume discretization is a crucial component of a dynamic greenhouse simulation.

Discretization turns continuous characteristics, variables, models, or functions into discrete ones [17]. As shown in experimental greenhouses, this approach enables the dispersion of microclimate parameters in BES. The CFD tool has the capacity for parameter distribution because it has specified vertical and horizontal stratification/discretization functions in its operation. Although it is rarely used, TRNSYS is another program with functionality for discretization [16]. The TRNSYS thermal point is referred to as an “air node” by TRANSSOLAR Energietechnik [18], and the simulation of several air node zones is a sophisticated modeling capability. A stack of air nodes within one zone frequently depicts large volumes, such as those found in atriums. As a result, the top air node may be warmer than the bottom air node. TRNSYS is an acronym for transient system simulation, a software developed by the University of Wisconsin's Solar Energy Laboratory, one of the most popular software programs for greenhouse simulation [19]. Laghmich *et al.* and Baglivo *et al.* [16,20] have recommended the use of discrete volume BES (DVBES). Laghmich

*et al.* [20] reported that DVBES could reduce energy prediction error by 32 %. Hence, the significant advantage of using DVBES over BES has been that its prediction is more accurate. It also allows for the simulation of multiple thermal nodes. Ogunlowo *et al.* [19] studied the effect of envelope characters in TRNSYS DVBES. They found that using 3D geometry with a massless layer in TRNSYS 18 (the latest version) demonstrated a similar distribution with their corresponding experimental greenhouses, making it more accurate.

Crop presence in a greenhouse has been found to affect the energy balance of the greenhouse through evapotranspiration [9] and the temperature difference between the crop and its immediate surrounding air [21]. Hence, researchers have been found to integrate different crop models into BES models as energy gain or loss. For example, to accommodate different data availability, Blaney-Criddle, Radiation, FAO Penman-Monteith, and Pan Evaporation, methods were often selected to calculate reference crop evapotranspiration [16]. According to Baglivo *et al.* [16], Penman-Monteith is the most accurate model with the minimum possible error out of these methods. The simple conductive heat transfer has been modified and deployed by Shen *et al.* [21] in the case of the crop model based on temperature difference. These models have been particularly integrated with the TRNSYS BES model by Baglivo *et al.* [16], Ward *et al.* [9], and Shen *et al.* [21].

The proposed DVBES model in this study may be used to study the effect of integrating phase change materials (PCMs) in the greenhouse structure. Hence, it is important to look at the use of PCM and its benefits in greenhouse energy saving. According to Jayalath *et al.* [22], PCMs provide a practical method for increasing energy efficiency in buildings by delaying heat transfer during the day, storing energy, and releasing the stored energy during the night or a colder period. Additionally, building materials that integrate PCMs can store large amounts of thermal energy in an envelope of a structure with less structural mass than sensible heat storage [23]. Depending on whether the phase transition temperature is attained, the energy gain may be sensible storage, latent storage, or both. Experimental [24] and numerical [22,25,26] methods have been used in the past to evaluate the thermal performance of PCMs installed in buildings. Thermal performance investigations using various PCMs and installation techniques within a building envelope have become a reality because of BES software tools [22].

The most widely used BES tools, according to Mazzeo *et al.* [2], in their investigation of the most accurate PCM-BES tools, were IDA ICE, EnergyPlus, and TRNSYS. To mimic PCM behavior and assess the potential to lower heating and cooling loads inside an office building for several climates in Italy, Cornaro *et al.* [27] developed a PCM wall implemented in IDA ICE. In the cases of Jayalath *et al.* [22] and

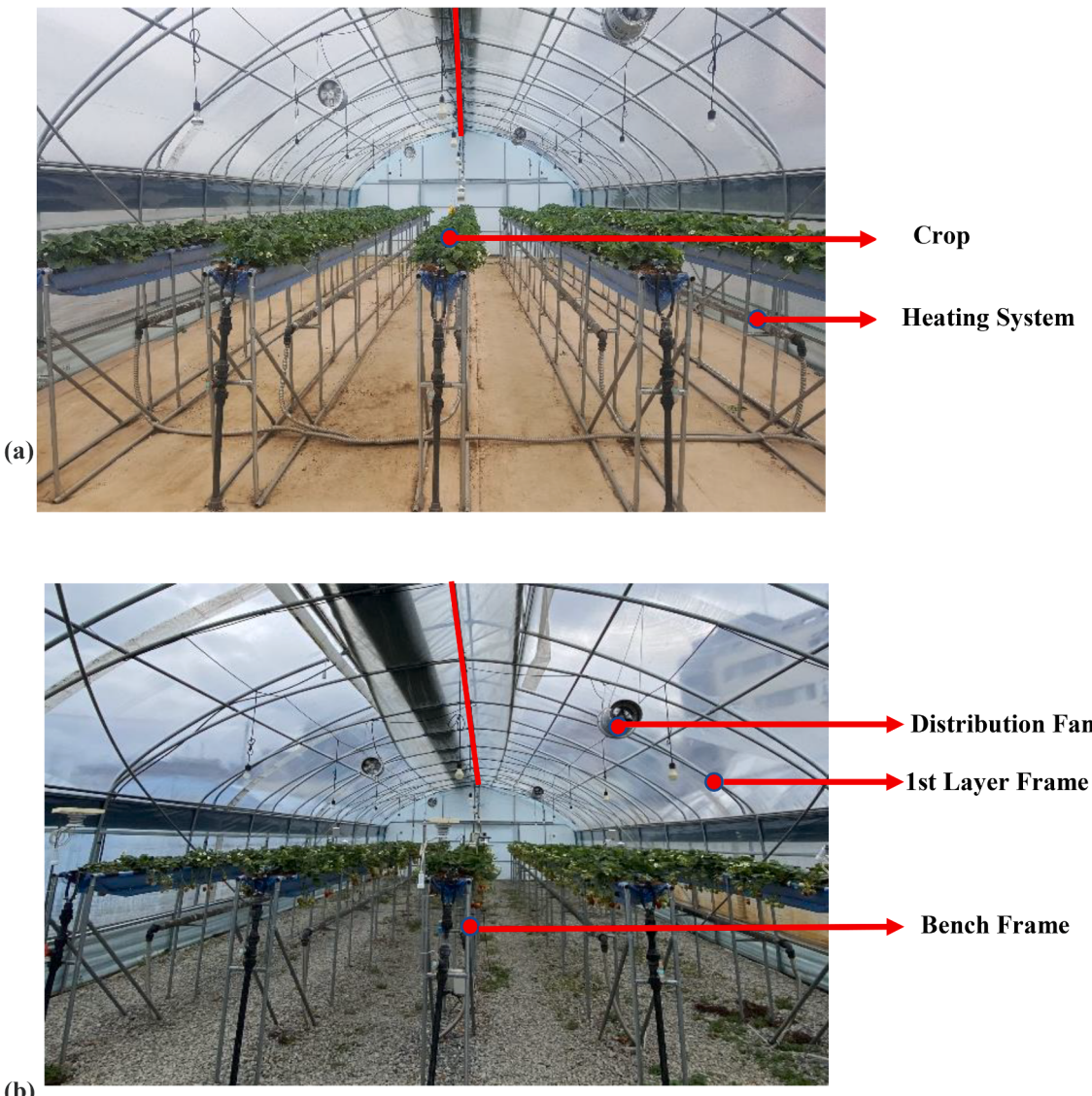


**Fig. 1.** Experimental greenhouses showing thermal screen positions and design features in (a)RGH and (b) QGH.

Panayiotou et al. [28], a PCM wall known as "Type 1270" was created, validated, and utilized in TRNSYS 16 to assess the thermal efficiency of an Australian single-story home. Types 260, 241, and 204, each coupled with Type 56 (Multizone Building), were created by Virgone et al., Schranzhofer et al., and Poulad et al. [29–31], respectively, to simulate test cells with PCM in the walls. However, when the PCM layer is integrated into walls in contact with both boundary surfaces inside a thermal zone, the "Types" in TRNSYS 16 were created to interact with the Type 56. Since the PCM layer immediately interacts with the thermal air node and the wall connected to the outer environment, the "Types" cannot be employed [2]. Ogunlowo et al. [32] created a PCM component in TRNSYS in 2023 as a result of this. The component's output (energy stored) can be adjusted as gain in the DVBES model and connected to the DVBES model.

In the past, performance evaluation of greenhouses was conducted by considering only the energy demand with no or less attention to the crop output (yield). However, the profit margin depends on how much revenue is generated with fewer expenses. In other words, a farmer's satisfaction will be reducing energy costs without compromising the crop yield. Due to the lack of studies using on-farm experimental data of growth-pattern responses to environmental factors due to difficulty in continuous monitoring and direct management of crops, Sim et al. [33] developed a predictive strawberry yield model based on greenhouse environmental and growth data. They used average daytime air temperature, soil temperature, relative humidity (RH), vapor pressure deficit (VPD), and photoactive radiation (PAR) to predict the greenhouse strawberry yield. However, these parameters are measured data and not predicted data. TRNSYS is commonly used to predict greenhouse energy demand [6,8,9], air temperature, and RH [19,34,35]. Setting other outputs can be difficult or not possible at the present level of research in TRNSYS. If greenhouse strawberry yield is to be predicted, attention must be directed to the easily predictable parameters.

Lacking in literature is a numerical evaluation of greenhouse based on its energy utilization and effect on crop yield. Also lacking is a PCM-cum-crop integrated DVBES model capable of setting the required number of inputs for a predictive crop yield model. Therefore, this study aims to simulate and analyze the energy dynamics within a greenhouse environment and then use the output temperature and RH to predict strawberry yield.

The primary objective of this research is to establish a base case scenario encompassing the energy behavior of the greenhouse and its direct influence on the yield of strawberries (*Seolhyang* sp.). The secondary objectives are to develop a ventilated DVBES that predicts a greenhouse's energy demand, temperature, and RH and a predictive strawberry yield model from the predicted temperature and RH that indicates the strawberry yield. Strawberry cultivation was chosen due to its economic significance [36,37] and high sensitivity to environmental conditions [37,38], making strawberries an ideal crop for studying the correlation between energy management and yield. By examining the relationship between energy consumption and crop productivity, opportunities for energy optimization can be identified, and sustainable greenhouse management practices can be developed by identifying a system with the least energy demand with the highest possible yield.

The outcomes of this study should be able to provide valuable insights into the energy performance of greenhouses and their impact on crop yield. Moreover, the findings will serve as a foundation for further research on optimizing energy consumption in greenhouse environments, leading to more sustainable and efficient agricultural practices. Ultimately, this research should also be able to contribute to advancing knowledge in sustainable agriculture and facilitate the transition toward a greener and more resource-conscious future.

This paper was subdivided into four sections. Section one introduces the study by looking into the background, literature, and objectives. Section two provides materials and methods used to achieve stated goals. Section three presents the results and duly discussed. The last section summarily presents the main findings of the study.

**Table 1**  
Feature description and control settings.

S/ No.	Feature	Description	Capacity
1	Crop	Strawberry plant ( <i>Seolhyang</i> sp.)	650 plant population (minimum)
2	Support frames	1. First layer frame: a 40-mm-diameter galvanized pipe with 2-mm thickness. Bench frame: a 12-mm galvanized pipe with 1-mm thickness. Potential container for PCM filling	0.163 m <sup>3</sup> PCM volume and 0.0817 m <sup>3</sup> pipe volume
3	Heating system	A stainless-steel diesel boiler connected to a heat exchanger	0.09 m <sup>3</sup>
4	Distribution fans	Four horizontal fans to mix greenhouse air	25 m <sup>3</sup> /s
5	Control	1. Ventilation: (a) vents open: 23 °C; (b) vents close: 22 °C Heating: (a) boiler start: 7.5 °C; (b) boiler stop: 8 °C; (c) pump start: 7.5 °C; (d) pump stop: 8 °C Envelope: (a) first layer open: 9:30; (b) first layer close: 17:30; (c) TS open: 9:00; (d) TS close: 18:00	
6	Location	Daegu (35.53°N, 128.36°E) 48 m above sea level	
7	Orientation	East-West (90°)	

## 2. Materials and methods

This section describes the experimental greenhouses, DVBES model development and validation, strawberry yield model development and validation, and strawberry yield prediction based on the predicted greenhouse temperature and RH data.

### 2.1. Description of experimental greenhouses

The experimental greenhouses are located at Kyungpook National University's Smart Farm Center in Daegu, South Korea. The first layer is an 18 × 6.5 m floor area, enclosed in a 24 × 7 m second layer. Both layers are enveloped by a polyolefin (PO) screen from 6 p.m. to 9 a.m., with an additional thermal screen (TS) layer on top of the first layer. During the day (from 9 a.m. to 6 p.m.), the PO screens on the first layer are rolled up, making the greenhouse single-layered during this period. Fig. 1 shows the design features of the experimental greenhouses R and Q (names are simply for identification and distinction), later referred to as R-greenhouse (RGH) and Q-greenhouse (QGH), respectively. The greenhouses are typical double-layer, single-span greenhouses for growing strawberry plants. Each greenhouse consists of five 14-m-long benches to support the crop substrate. Table 1 describes each feature and states the control settings of the greenhouses. Fig. 2 shows the floor dimensions of the greenhouses and the position of the sensors. To ensure that the conditions of the two greenhouses differ, RGH has its TS at the center, whereas QGH has its TS 5° toward the north end of the greenhouse. Moreover, QGH and RGH are characterized by a layer of gravel and a layer of polyvinyl on the floor, respectively.

As shown in Fig. 2, nine Hobo onset U23-002 sensors with a sensitivity of ± 0.21 °C (from 0 °C to 50 °C) and ± 2.5 % (from 10 % to 100 % RH) were installed to record the air temperature and RH. Furthermore, three Kipp and Zonen pyranometers (CMP3 model) with a sensitivity of < 5 % and –10 °C to 40 °C and a spectral range of 300–2800 nm were used to record the solar radiation (SR) at the north, center, and south end of the greenhouses. An Apogee infrared radiometer surface temperature sensor (SI-131-SS model) with a sensitivity of ± 0.3 °C (ranging from –30 to 65 °C) was installed to measure the leaf surface temperature.

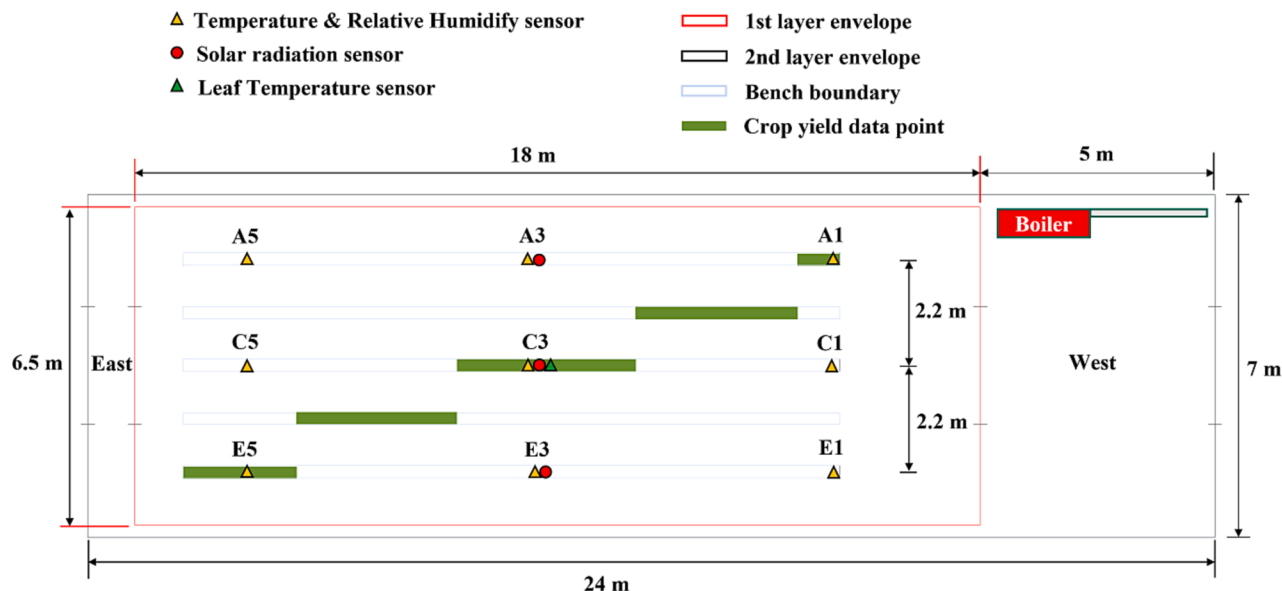


Fig. 2. Floor dimension of the experimental greenhouses and sensor location.

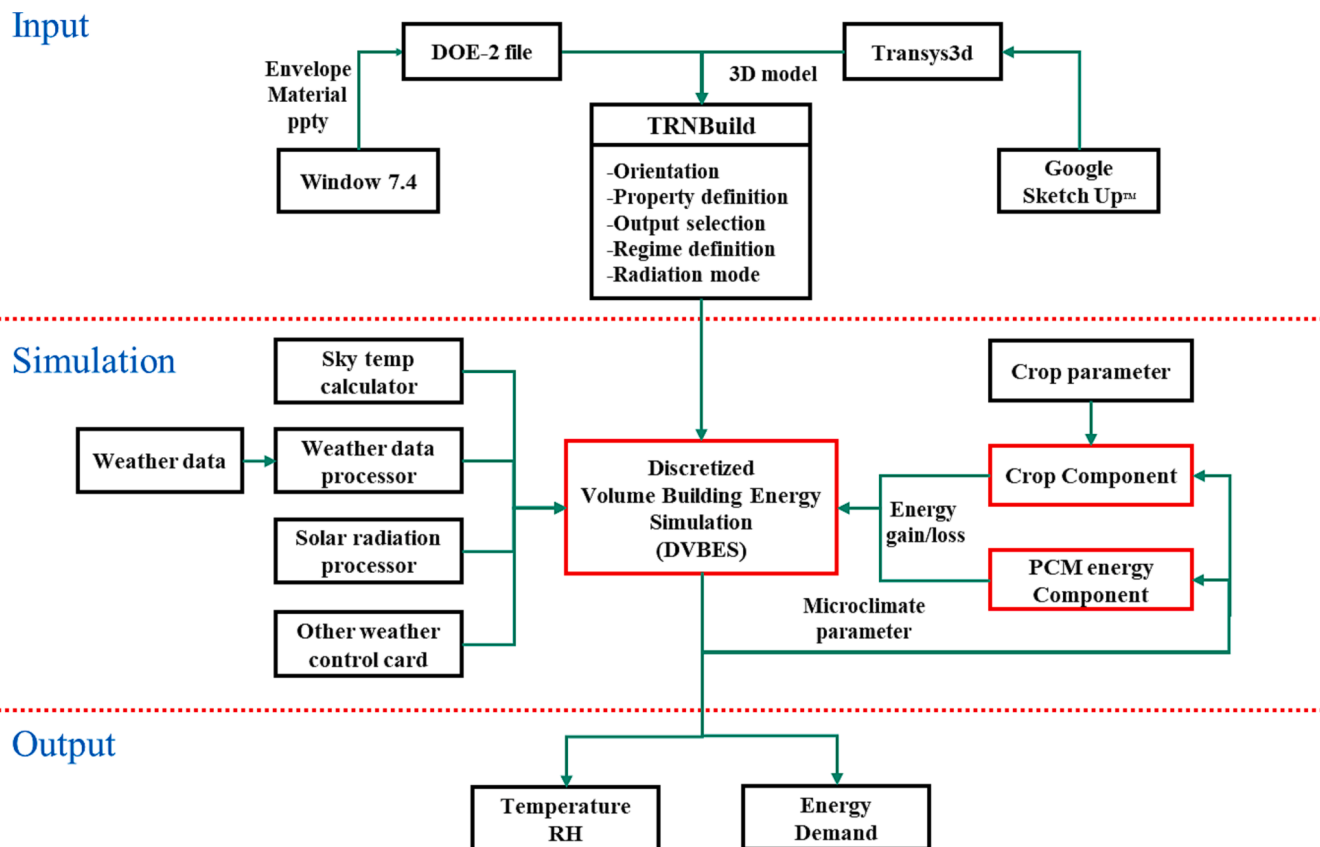
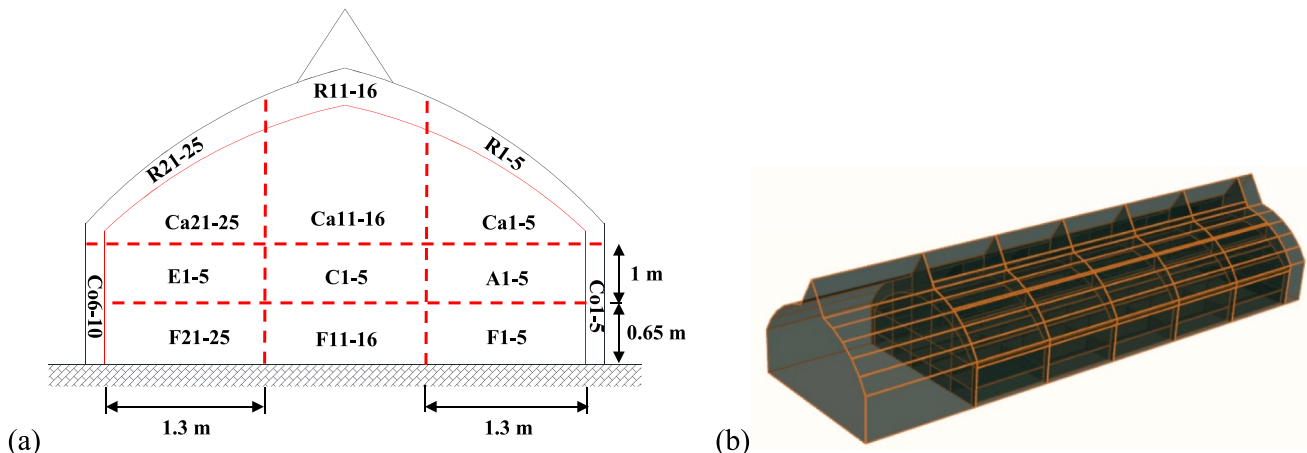


Fig. 3. Flowchart of the mechanism of the TRNSYS 18 simulation model.

## 2.2. Greenhouse model development and validation

This study proposes a DVBES to predict the energy demand, temperature, and RH effectively and accurately within a greenhouse. This requires accurately modeling the features in the experimental greenhouses and the envelope materials. Fig. 3 shows the flowchart for the simulation of energy demand, temperature, and RH in the TRNSYS 18 simulation model. The flowchart is divided into input, simulation, and output.

The input consists of TRNBuild —a TRNSYS tool for building description; SketchUp – a building 3D software developed by Trimble incorporation; and Window 7.4 software developed by Lawrence Berkeley National Laboratory (LBNL.) TRNBuild defines the building's required envelope characteristics and regime, including the geometry of the structure, radiation mode, infiltration and ventilation, number of zones/air nodes, and thermal and moisture capacitance of the zone/air node. The geometry of the greenhouse can be manually entered into



**Fig. 4.** Front view (a) and 3D isometric view (b) of the model greenhouse as designed in SketchUp.

**Table 2**  
Regime definition in TRNBuild.

Area	Air node	Volume (m <sup>3</sup> )	Capacitance (kJ. K <sup>-1</sup> )	Ref. floor area (m <sup>2</sup> )
Floor	F1-25	3.04	18.26	4.68
Crop	A1-E5	4.68	28.08	4.68
Canopy	Ca1-5, Ca21- 25	3.02 6.58	3.63 7.89	4.68
	Ca6-10, Ca16-20 Ca11-15	7.60	9.12	
Roof	R1-5, R21-25 R6-10, R16- 20 R11-15	3.56 3.30 6.45	4.28 3.96 7.75	7.16 4.99 4.70
Corridor	Co1-10	1.49	1.78	0.90
West	West	122.99	737.87	35.00
East	East	24.60	29.52	7.00

TRNBuild or imported into SketchUp as a *.idf* file format. Zones and geometry are generated when a Trnsys3d file (*.idf*) is loaded from SketchUp into TRNBuild. The geometry mode is automatically set to 3D data and thus, a 3D geometry. The Window 7.4 software generates a *DOE-2* file containing information about the glazing materials, then imported into TRNBuild.

The simulation consists of the weather components, DVBES, crop component, and PCM component. The weather components are the sky temperature calculator – which calculates the sky temperature from weather parameters such as ambient temperature and RH; the weather data processor – which reads the data from the data file; the solar radiation processor – which calculates the solar radiation incidence on every angle; and other components such as psychometric and orientation calculators. The DVBES integrates all other components, further described in section 2.2.1. The crop and PCM components calculate the energy gain or loss from the crop and PCM, respectively. They are further described in the following sub-sections.

Finally, the output parts are simply output components that present the intended outputs as a *.text* or *.xls* files, depending on the user preference. In this case, the results are the greenhouse temperature, RH, and heating energy demand.

### 2.2.1. The DVBES model

This study adopts the model developed by Ogunlowo et al. [19], who developed a nonventilated DVBES and defined all envelope characters in their research. In this case, 112 discrete air nodes were created and ventilated per the operation of the experimental RGH. Fig. 4 shows the front view and the 3D model of the stacked air node as developed in

**Table 3**  
Characteristics of envelope materials as used in TRNBuild.

Surface type	Category	Material	Thickness (m)	U-value (W.m <sup>-2</sup> K <sup>-1</sup> )	Layer type
Opaque	Ext_Wall/Roof	Steel	0.05	5.769	Massive
	Adj_Wall	Steel	0.04	5.792	Massive
	Adj_Wall2	Air layer	0.00	2.948	Massless
	Adj_Wall3	PO-MW-PO	0.05	0.999	Massive
	Adj_Ceiling	Steel	0.04	5.792	Massive
	Adj_Ceiling2	Air layer	0.00	2.948	Massless
	Adj_Ceiling3	PO-MW	0.036	0.878	Massive
	Ground_Floor	Under_floor	0.15	2.04	Massive
	Adj_Window	PO		ST (0.08), SR (0.10), VRT (0.89), VRR (0.08), TRT (0.18), TRE (0.79), TC (0.33), T(0.10)	
Glazing	Adj_Window1/ 2	PO-MW "No glazing"	(9 am–6 pm) (6 pm–9 am)		

Ext, external; Adj, adjacent; PO, polyolefin; MW, mineral wool; ST, solar transmittance; SR, solar reflectance; VRT, visible radiation transmittance; VRR, visible radiation reflectance; TRT, thermal radiation transmittance; TRE, thermal radiation emission; TC, thermal conductivity (W.m<sup>-1</sup>K<sup>-1</sup>); T, thickness (mm).

SketchUp (a building 3D model software developed by Trimble Incorporation). In Fig. 3a, the red dotted lines, the solid line, and the solid black line represent the air layers separating adjacent air nodes, the first layer envelope, and the second (external) layer envelope. Tables 2 and 3 present the properties and the regime definition of the discrete air node, respectively, as defined in TRNBuild – an interface for the creation and edition of non-geometry information required by TRNSYS.

Based on the principle of energy conservation, the energy demand to maintain a greenhouse discrete set temperature can be expressed as heat exchange between the inside design components and the ambient, as shown in Eq. (1) [18]. The summation of the discrete makes the total energy demand of the DVBES.

$$Q_{D\text{-Demand}} = Q_{air} + Q_{inf} + Q_{vent} + Q_{coup} + Q_{trans} + Q_{wgain} + Q_{sol} + Q_{solair} + Q_{gint} \quad (1)$$

where  $Q_{air}$  is the change of internal energy of zone calculated with capacitance of air,  $Q_{inf}$  represents the infiltration gains,  $Q_{vent}$  represents the ventilation gains,  $Q_{coup}$  represents the coupling gains,  $Q_{trans}$  is the transmission into the surface from the inner surface node,  $Q_{wgain}$  represents the wall gains,  $Q_{sol}$  represents the absorbed solar gains on all inside surfaces of zones,  $Q_{solair}$  is the convective energy gain of zone due to the

transmitted SR through external windows which is transformed immediately into a convective heat flow to internal air, and  $Q_{gint}$  represents the internal gains,  $Q_{crop} + Q_{pcm}$ .

### 2.2.2. Crop component

The evapotranspiration and crop equation used by Baglivo *et al.* and Shen *et al.* [16,21], respectively, were adopted to account for the contribution of the crop to the system energy. The crop component is a nonstandard component developed in TRNSYS based on Eqs. (2)–(5):

$$ET_o = \frac{0.408 * \Delta * (R_n - G) + \gamma \frac{37}{T_a + 273} u_2 (e_o - e_a)}{\Delta + \gamma (1 + 0.34 u_2)} \quad (2)$$

$$m_{ETO} = ET_o * A_{sub} * \rho * 10^{-3} \quad (3)$$

$$Q_{ET} = m_{ETO} * (r_o + c_v * T_a) \quad (4)$$

$$Q_{crop} = 2 * S_g * LAI * \rho * c_{air} * \frac{(T_a - T_{leaf})}{r_b} \quad (5)$$

### 2.2.3. Phase change materials (PCM) component

The first layer (FLF) and bench frames (BF) shown in Fig. 1 could be used as a container for PCMs. Studies have shown that PCM could reduce energy consumption. Therefore, a PCM-in-container component developed in TRNSYS by Ogunlowo *et al.* [32] was adopted. The energy equation of the component was temperature based, as shown in Eq. (6). The FLF and BF were “no-fill” in this study.

$$Q_{pcm} = [\rho_s V_s c_s (T_f - T_i) + \rho_p V_p L + \rho_l V_l c_l (T_f - T_i)] + \rho_c V_c c_c (T_f - T_i) \quad (6)$$

Boundary conditions

$$Q_{pcm} = \rho_s V_s c_s (T_f - T_i) + \rho_c V_c c_c (T_f - T_i) (T_i < T_m)$$

$$Q_{pcm} = \rho_p V_p L + \rho_c V_c c_c (T_f - T_i) (T_f = T_i = T_m)$$

$$Q_{pcm} = \rho_l V_l c_l (T_f - T_i) + \rho_c V_c c_c (T_f - T_i) (T_i > T_m)$$

### 2.2.4. Model validation

Experimentation was conducted using the RGH to validate the model. The temperature, RH, and SR of the RGH's microclimate (sensors' location are shown in Fig. 1), ambient temperature, wind speed, wind direction, horizontal SR, and pressure were recorded every 10 min.

In the simulation, as shown in Fig. 2, all components were linked, and the ambient recorded data collected during the winter season (December 2 to February 27, 2023) were used. The outputs of the simulation—heating demand, air temperature, and RH—were compared with the boiler fuel consumption, microclimate temperature, and RH from the experimental RGH, using the following metrics: coefficient of determination ( $R^2$ ) [2], root mean squared error (RMSE) [22,27], normalized mean bias error (NMBE), and coefficient of variance of the root mean squared error (CVRMSE). According to ASHRAE [39], CVRMSE tests how well the model recreates the data and is also an indication of random error. NMBE tests how biased the model is in predicting outputs over the period the model was developed. In addition, ASHRAE [40] reported that a model is considered calibrated if NMBE and CVRMSE are  $< 5\%$  and  $< 15\%$ , respectively, for a monthly data, or if NMBE and CVRMSE are  $< 10\%$  and  $< 30\%$ , respectively, for an hourly data.

$$R^2 = 1 - \frac{\sum_{i=1}^N (Exp_i - Sim_i)^2}{\sum_{i=1}^N (Exp_i - Av)^2}, Av = \frac{1}{N} \sum_{i=1}^N Exp_i \quad (7)$$

**Table 4**

Plant population within the data points during the winter of the planting seasons.

Collection point	RGH		QGH	
	2021–2022	2022–2023	2021–2022	2022–2023
A1	3	5	2	4
C3	34	32	35	35
E5	23	23	22	24

$$RSME = \sqrt{\frac{1}{N} \sum_{i=1}^N (Exp_i - Sim_i)^2} \quad (8)$$

$$NMBE = \frac{\sum_i^N (Exp_i - Sim_i)}{(N - 1) * Av} * 100\% \quad (9)$$

$$CVRMSE = \sqrt{\frac{\sum_{i=1}^N (Exp_i - Sim_i)^2}{N - 1}} * 100\% \quad (10)$$

$Av$  is the mean of the experimental value,  $Exp_i$  is the experimental value,  $Sim_i$  is the simulated value, and  $N$  is the data population.

### 2.3. Strawberry yield model

There is a need for a model that takes in predicted greenhouse microclimate parameters as inputs and sets out the yield as output to evaluate the performance of greenhouse energy demand and direct influence on crop yield. Sim *et al.* [33] used a “Seolhyang” cultivar to develop an empirical strawberry yield model (Eq. (11)) based on experimentally measured greenhouse average day air temperature (ADAT), soil temperature (ST), RH, photoactive radiation (PAR), and calculated vapor pressure deficit (VPD) data. However, adopting this model comes with its inadequacies. For instance, the strawberries were planted on the ground, unlike planting using the BF used in this study; hence, the input, ST, would not have been suited in this case. Moreover, the goal is to calculate the weekly yield without accumulation, which the model could not. In contrast, to develop a yield prediction model for greenhouse-grown lettuce, Lin [41] used weekly data, and as the crop grew, the most recent weekly data were added. Therefore, the method used by Lin [41] was adopted in this study.

#### 2.3.1. Data collection and preparation

Two harvest seasons were used in this study, i.e., winter of 2021–2022 and 2022–2023. The output data, yield, input data, temperature, RH, and SR were measured at the points shown in Fig. 2, while the VPD was calculated from the temperature and RH. The data were collected from the two experimental greenhouses (RGH and QGH) for ten weeks. With three collection points in each greenhouse and two seasons of harvest for 12 weeks, the total data points amount to 144. Table 4 presents the plant population at the data points. The yield data were recorded every week, whereas the temperature ( $^{\circ}\text{C}$ ), RH (%), and SR ( $\text{W.m}^{-2}$ ) were recorded every 10 min and then later arranged for every week. Hobo Onset U23-002 sensors with a sensitivity of  $\pm 0.21\text{ }^{\circ}\text{C}$  (from  $0\text{ }^{\circ}\text{C}$  to  $50\text{ }^{\circ}\text{C}$ ) were used to record the temperature and RH data. Kipp and Zonen pyranometers (CMP3 model) with a sensitivity of  $< 5\%$  and  $-10\text{ }^{\circ}\text{C}$  to  $40\text{ }^{\circ}\text{C}$  and a spectral range of 300–2800 nm were used to record the SR. CAS electronic weighing scales, model PB and CUW2200H, with a maximum display of 60 kg and 2.2 kg, respectively, were used to measure the yield.

$$Y(\text{kg.}10\text{a}^{-1}) = -52771.5 + 1194.2 \cdot \text{ADAT} - 2223.2 \cdot \text{ST} + 685.0 \cdot \text{RH} + 56896.3 \cdot \text{VPD} + 78.2 \cdot \text{PAR} \quad (11)$$

Where Y is yield in kg per 10 of acre ( $\text{kg.}10\text{a}^{-1}$ ); ADAT is average daily air temperature ( $^{\circ}\text{C}$ ); ST is soil temperature ( $^{\circ}\text{C}$ ); RH is relative humidity ( $^{\circ}\text{C}$ ); VPD is vapor pressure deficit ( $\text{kPa}$ ); and PAR is photoactive radiation ( $\mu\text{mol.m}^{-2}.s^{-1}$ ).

The procedure for data preparation is as follows:

1. The weekly yield from each point is divided by the plant population to get the yield per plant per week ( $\text{kg.plant}^{-1}\text{week}^{-1}$ ).
2. While the yield data are arranged weekly, the temperature, RH, VPD, and daily SR for the new week is added to the data of the previous week in line with the method by Lin [41].
3. The variant of temperature and RH are made as follows: average nighttime temperature (X1), percentage optimum nighttime temperature (X2), average daytime temperature (X3), percentage optimum daytime temperature (X4), average nighttime RH (X5), percentage optimum nighttime RH (X6), average daytime RH (X7), percentage optimum daytime RH (X8), average nighttime VPD (X9), percentage optimum nighttime VPD (X10), average daytime VPD

(X11), percentage optimum daytime VPD (X12), and the daily SR (X13).

Ogunlowo et al. [15] reported that the optimum nighttime and daytime temperature range for strawberry is  $8^{\circ}\text{C}$ – $13^{\circ}\text{C}$  and  $18^{\circ}\text{C}$ – $23^{\circ}\text{C}$ , respectively, and the optimum nighttime and daytime RH range is 60 %–75 %.

### 2.3.2. Statistical analysis and model validation

To develop the yield model and determine the relationship between the variables (X1, X2, ..., X13) and yield (Y) and the variables' contribution to the yield, multiple regression analysis—a common tool used by Sim et al. and Odey et al. [33,42], among others—was performed using Minitab software (Version 20.3). The data from the two harvest seasons were divided into two sets. The data from all points in the first season and points A1 and E5 were used as a training set, and the data from point C3 in the second season was used as a test set.  $R^2$ , NMSE, and RSME were used to validate the developed model.

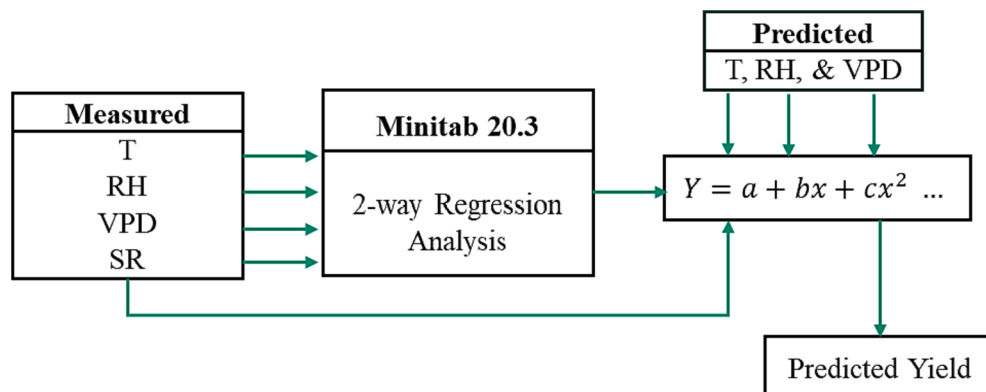


**Fig. 5.** Flowchart of strawberry yield prediction from predicted greenhouse microclimate variables.

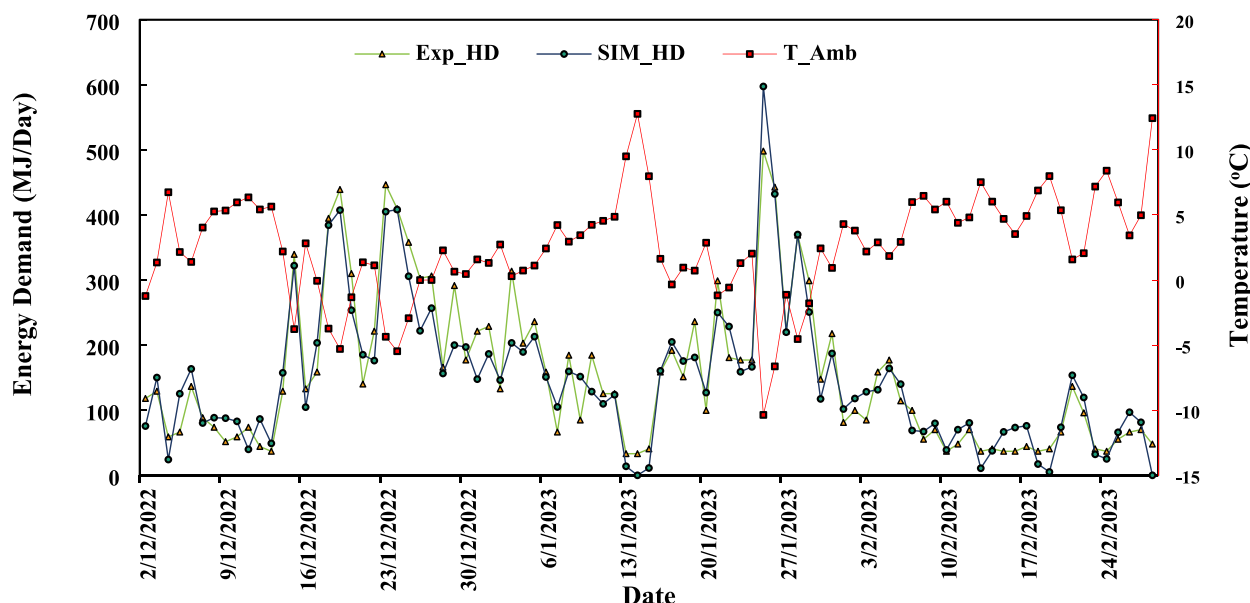


**Fig. 6.** Experimental and simulated daily heating demand during the experimental period.

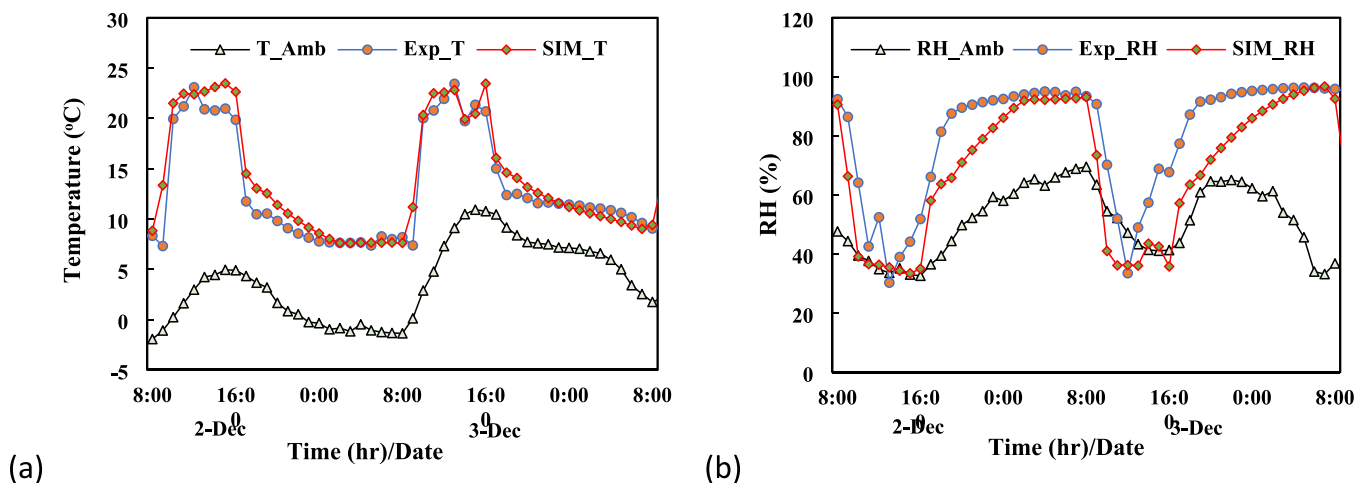


Fig. 7. Comparison of the experimental and simulated temperature (a) and RH (b).

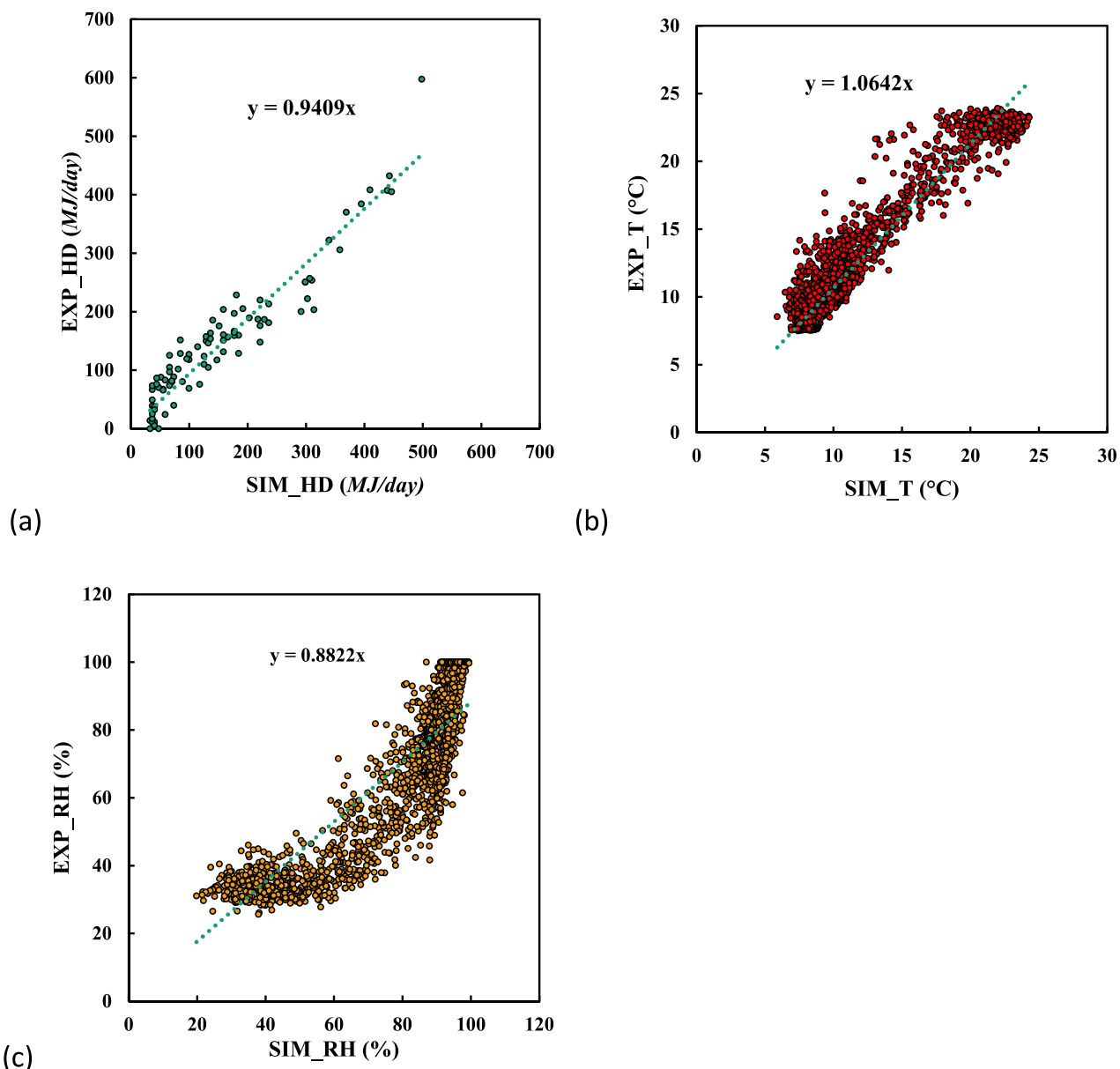


Fig. 8. One-to-one plot of experimental against simulated daily energy demand (a), hourly temperature (b), and hourly RH (c).

**Table 5**  
Summary of validation results.

	R <sup>2</sup>	RSME	NMBE	CVRMSE
Energy	0.90	36.70 MJ	3.28	21.99
Temperature	0.89	1.74 °C	-7.29	14.24
RH	0.50	14.62 %	12.49	18.46

#### 2.4. Establishing the base case

After confirming the accuracy of the models, i.e., the DVBES and the strawberry yield model, the base case energy demand and strawberry yield of RGH were established by deploying the models. Fig. 2 shows the flowchart to achieve the energy demand, whereas Fig. 5 shows the flowchart to achieve the predicted yield. Fig. 5 shows how the measured data was received by Minitab 20.3 software. Using a two-way regression analysis, the software generates the empirical model for future prediction of the strawberry yield. The greenhouse simulation was carried out for the second season of winter from the second week of December 2022, when the crop harvest started, to the last week of February 2023.

The total heating demand for this period was recorded as the base case heating demand. Whereas, apart from the heating demand, the predicted temperature, RH from the simulation, and the calculated VPD were used as input (as shown in Fig. 5) for the newly developed strawberry yield model to predict the strawberry yield of the simulated period.

### 3. Results and discussion

#### 3.1. Energy, temperature, and RH prediction accuracy

Figs. 6 and 7 (a and b) compare the experimental and simulated heating demand (Exp\_HD and Sim\_HD), temperature, and RH, respectively. For visual clarity, two days of the plot were used in Fig. 7. As shown in Fig. 6, on January 25, the heating demand was observed to be highest when the average daily ambient temperature (T\_Amb) was the lowest ( $-10^{\circ}\text{C}$ ). In contrast, on January 14 and February 28, the heating demand was observed to be least when the average T\_Amb was  $12^{\circ}\text{C}$ . This indicates the adequate response of the model to the external and

driving forces. As shown in Fig. 7, while the temperature plot (Fig. 7a) shows an almost perfect fit, the RH plot (Fig. 7b) shows a lag between the experimental and simulated values.

Fig. 8 shows the one-to-one scatterplots of the experimental heating energy, temperature, and RH against the simulated parameters. A very strong deviation of 50%–80% can be seen within the RH data (Fig. 8c).

Table 5 summarizes the model's accuracy to predict the energy demand, temperature, and RH. For the energy demand, the R<sup>2</sup> value of 0.90 suggests a strong correlation between the simulated and experimental energy values. According to Casella [43], R<sup>2</sup> is a measure of goodness of fit of a model with a value of 1 indicating a perfect fit. Hence, a value of 0.90 indicates a very good fit. However, the RSME value of 36.70 MJ (about 1 L of diesel fuel [44]) indicates a relatively high average magnitude of prediction errors. The NMBE value of 3.28 % indicates a slight bias in the predictions, while the CVRMSE value of 21.99 % suggests moderate variation in the prediction errors. The NMBE and CVRSME are < 10 % and 30 %, respectively, indicating that the model does not require calibration before deployment [39].

A similar situation occurred in temperature. The R<sup>2</sup> value of 0.89 indicates a strong correlation between the simulated and experimental temperature values, suggesting a good fit between the experimental and simulated value [43]. The RSME value of  $1.74^{\circ}\text{C}$  indicates a relatively low average magnitude of prediction errors, the NMBE value of  $-7.29\%$  indicates a significant negative bias in the predictions, and the CVRMSE value of 14.24 % suggests a moderate level of variation in the prediction errors. The NMBE and CVRSME are also < 10 %.

However, in the RH situation, the R<sup>2</sup> value of 0.50 indicates a moderate correlation between the simulated and experimental RH values, suggesting a fair fit between the experimental and simulated value [43]. The RSME value of 14.62 % represents a relatively low average magnitude of prediction errors, the NMBE value of 12.49 % indicates a moderate positive bias in the predictions, and the CVRMSE value of 18.46 % suggests a reasonable variation in the prediction errors. NMBE was slightly above the recommended value of 10 %, whereas the CVRSME was lower than 30 %. The RSME value of 14.62 % was also similar to that reported by Mashonjowa *et al.* [34] but with a lesser R<sup>2</sup> value (0.57). The moderate correlation (R<sup>2</sup>) and relatively low RSME for RH indicate a reasonable accuracy level.

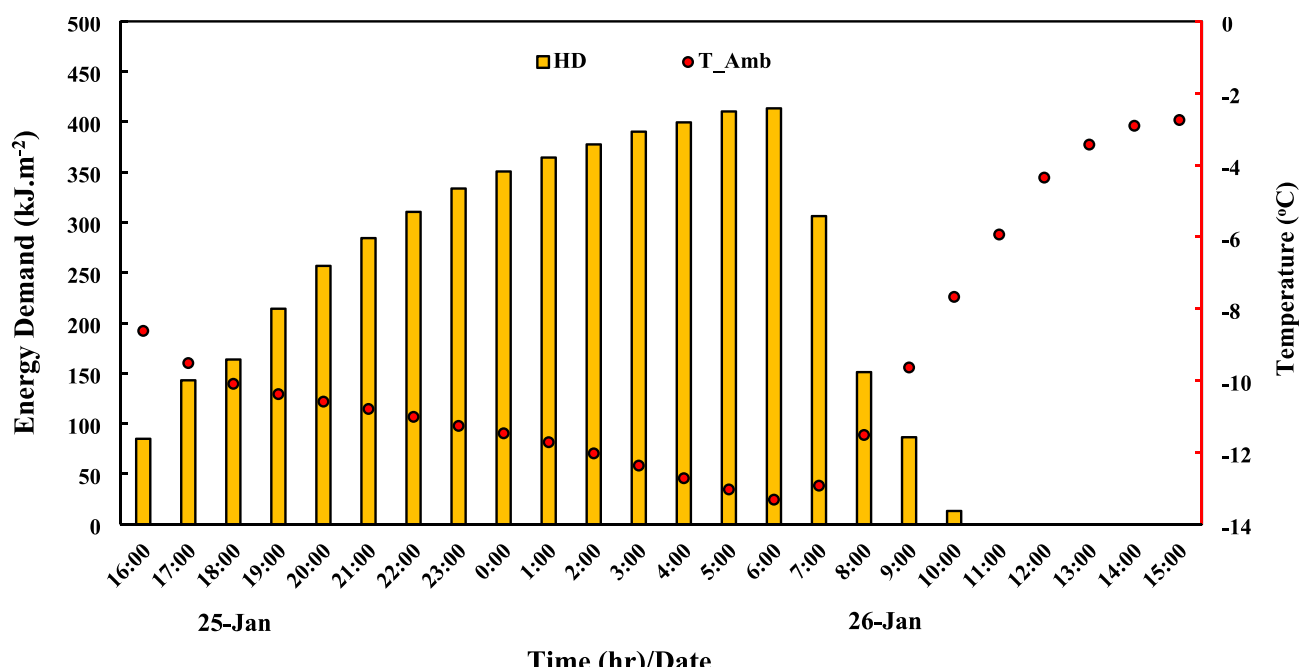


Fig. 9. Energy demand on the coldest day.

**Table 6**

Validation variables and metrics of the strawberry yield.

Week	X1	X2	X8	X13	E_Y	P_Y	R <sup>2</sup>	RSME	NMBE
1	9.880	85.238	33.333	197.955	0.011	0.001	0.978	0.008 kg	8.936 % (<10 %)
2	9.651	86.857	35.238	202.730	0.021	0.005			
3	9.507	88.095	34.921	206.597	0.002	0.012			
4	9.530	89.252	34.014	209.216	0.005	0.014			
5	9.572	87.976	33.333	203.733	0.017	0.014			
6	9.499	88.889	32.099	209.768	0.014	0.020			
7	9.460	89.524	30.635	217.934	0.023	0.024			
8	9.532	89.524	30.159	225.271	0.029	0.022			
9	9.613	89.841	30.291	220.233	0.022	0.019			
10	9.729	89.451	29.060	225.154	0.019	0.017			
				Total	0.162	0.148			

X1, average nighttime temperature ( $^{\circ}\text{C}$ ); X2, % optimum nighttime temperature (%); X8, % optimum daytime RH (%); X13, solar radiation ( $\text{W}/\text{m}^2$ ); E\_Y, measured yield (kg); P\_Y, predicted yield (kg).

In summary, the model demonstrates a good correlation with the actual values for all three variables, namely, energy demand, temperature, and RH, with the magnitude of prediction errors (RSME), bias (NMBE), and variation (CVRMSE) within the requirements and tolerances of its application. Therefore, the model is accurate enough for deployment, i.e., it is good enough to predict energy demand, temperature, and RH.

Fig. 9 shows the greenhouse energy demand on its coldest day (25th – 26th January 2023). The hourly energy demand increases steadily with the decrease in T\_Amb. The peak demand of  $413 \text{ kJ.m}^{-2}$  was recorded at 6 a.m. when the T\_Amb was  $-13^{\circ}\text{C}$ . Beyond this time, the greenhouse started obtaining solar energy, causing a rapid fall in the energy demand. As expected, the model followed the trend of natural phenomena.

### 3.2. Strawberry yield prediction accuracy

A regression model was developed to ascertain the effect of greenhouse microclimate temperature, RH, and SR on the “Seolhyang” cultivar of strawberry. The microclimate variables and yield data were computed using two-way interactions and quadratic terms, and these data were used to quantitatively estimate the relationships and variables’ contribution to the strawberry yield. The model was developed using significant variants of the greenhouse temperature RH, and SR.

The derived regression model is:

$$Y(\text{kg.plant}^{-1}.\text{week}^{-1}) = -0.276 + 0.0331 \times X1 + 0.00854 \\ \times X2 - 0.002363 \times X8 - 0.000111 \\ \times X13 - 0.000804 \times X1 \times X2 \quad (12)$$

Where Y is the predicted strawberry yield ( $\text{kg.plant}^{-1}.\text{week}^{-1}$ ), X1 is the average nighttime temperature ( $^{\circ}\text{C}$ ), X2 is the percentage optimum nighttime temperature (%), X8 is the percentage optimum daytime RH (%), and X13 is the SR ( $\text{W}/\text{m}^2$ ).

The yield variance is measured by the constant term in the equation if the microclimate variables remained constant for the period. It also accounts for factors such as fertigation and better farm management practices. The regression estimates show a strong relationship between the variables and the yield with  $p (\alpha=0.01) < 0.01$ , and the variables account for about 40 % of the changes in the strawberry yield, with  $R^2$  of 0.399, as shown in Fig. A.1. As illustrated in Eq. (12), a unit in the average night shift temperature will lead to an increase in yield by  $0.0331 \text{ kg.plant}^{-1}.\text{week}^{-1}$ , a unit in the change in percentage optimum nighttime temperature will increase the yield by  $0.00854 \text{ kg.plant}^{-1}.\text{week}^{-1}$ , a unit change in percentage optimum daytime RH will reduce the yield by  $0.002363 \text{ kg.plant}^{-1}.\text{week}^{-1}$ , a unit change in SR will reduce the yield by  $0.000111 \text{ kg.plant}^{-1}.\text{week}^{-1}$ , and a unit change in the product of the average and percentage optimum nighttime temperature will reduce the yield by  $0.000804 \text{ kg.plant}^{-1}.\text{week}^{-1}$ . Of the variables, X13 contributed the most variation to the yield. In contrast, X2 contributed the least variation (see Fig. A.2). The four variables

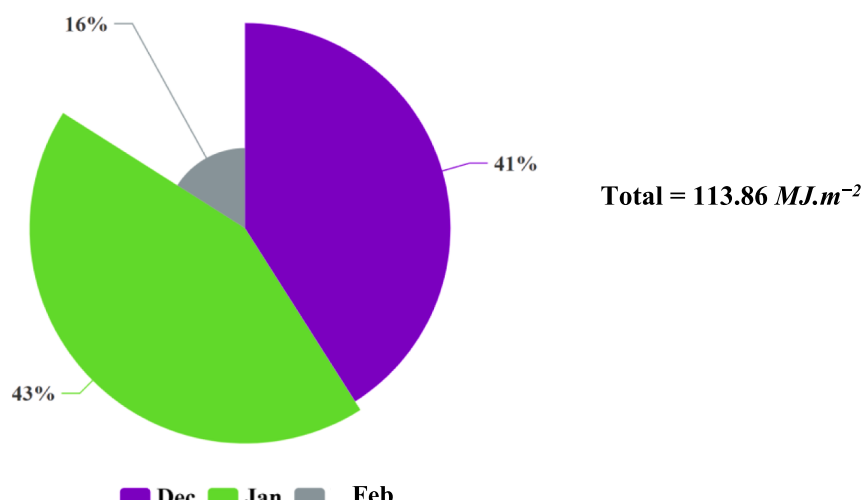


Fig. 10. Base case total energy demand for 3 months of 2022–2023 winter season.

**Table 7**

Base case yield, calculated from the DVBES predicted microclimate data.

Week	X1*	X2*	X8*	X13	Y*
1	9.601	58.095	7.937	220.544	0.046
2	9.526	61.429	9.524	203.684	0.048
3	9.026	49.841	10.582	181.095	0.042
4	8.844	45.476	9.524	234.185	0.033
5	8.813	45.333	9.206	223.744	0.035
6	8.971	46.825	8.201	223.624	0.039
7	9.071	46.939	7.710	162.868	0.046
8	8.990	45.238	7.738	253.772	0.034
9	8.999	44.868	7.584	283.802	0.031
10	9.142	45.619	7.460	286.597	0.031
11	9.230	48.398	8.081	180.811	0.045
12	9.352	50.238	8.201	273.724	0.035
			Total		0.466

\*: Predicted data.

conform with the report by Tang *et al.* [37], indicating that daytime shading and nighttime heating affect the strawberry yield. In other words, SR and nighttime temperature affect the strawberry yield.

The test data presented in Table 6 was used to check the deployability of the model. The  $R^2$  value of 0.98 indicates a strong correlation between the predicted and measured yield values, suggesting a suggesting a good fit between the experimental and simulated value [43]. The RSME value of 0.008 kg indicates a relatively low average magnitude of prediction errors, and the NMSE value of 8.936 % indicates a moderate bias in the predictions. The NMSE value is less than the acceptable level of 10 %, suggesting a recommendation for deployment.

With this model, the weekly strawberry yield in a greenhouse can be

predicted if the average nighttime temperature, percentage optimum nighttime temperature, percentage optimum daytime RH, and solar radiation are known.

### 3.3. Base case energy demand and strawberry yield

Fig. 10 and Table 7 show the base case energy demand and strawberry yield for the winter season (December 2022–February 2023). Of the total energy demand ( $113.861 \text{ MJ.m}^{-2}$ ), the highest demand of  $48.914 \text{ MJ.m}^{-2}$  was recorded in January, followed by  $47.424 \text{ MJ.m}^{-2}$  recorded in December. The lowest energy of  $18.168 \text{ MJ.m}^{-2}$  was recorded in February. The peak hourly heating demand of  $0.413 \text{ MJ.m}^{-2}$  was recorded at  $-13^\circ\text{C}$  in January (a common peak period in winter as evidenced by Rasheed *et al.*, Baglivo *et al.*, and Cornaro *et al.* [8,16,27]). It is important to note that the predicted value presented in Table 7 is an ideal value; hence, it was higher than the measured value.

Greenhouse farming has become a critical component of modern agriculture, enabling the cultivation of crops in controlled environments irrespective of external weather conditions. However, one of the critical challenges associated with greenhouse farming is managing energy consumption, as creating and maintaining the optimal conditions for plant growth often requires significant energy inputs for heating, cooling, lighting, and other operations. This energy consumption contributes to operational costs and environmental impacts, such as increased greenhouse gas emissions and resource depletion. In this study, to establish a base case energy demand and strawberry yield, a ventilated DVBES model was developed. For possible future evaluation, the model was integrated with a PCM component, simulated under a no-fill scenario.

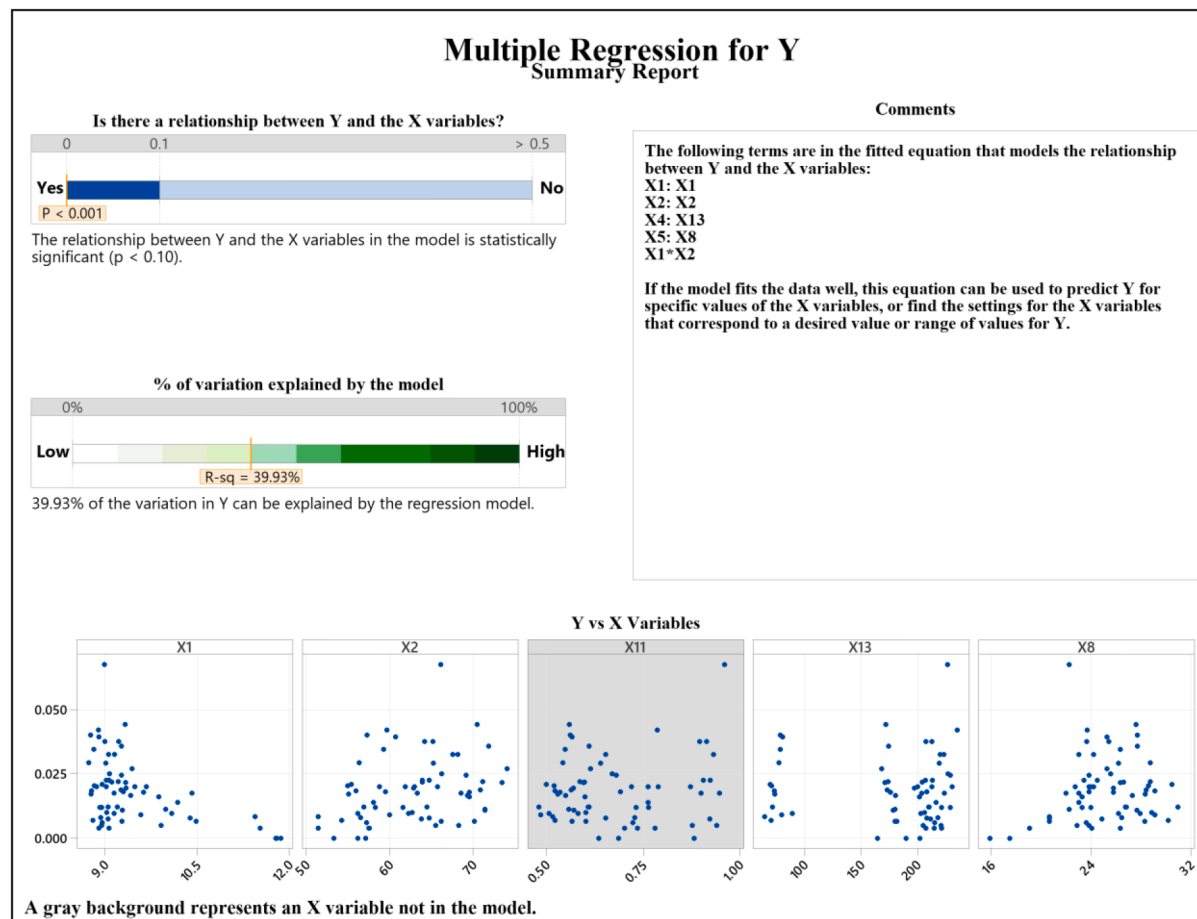
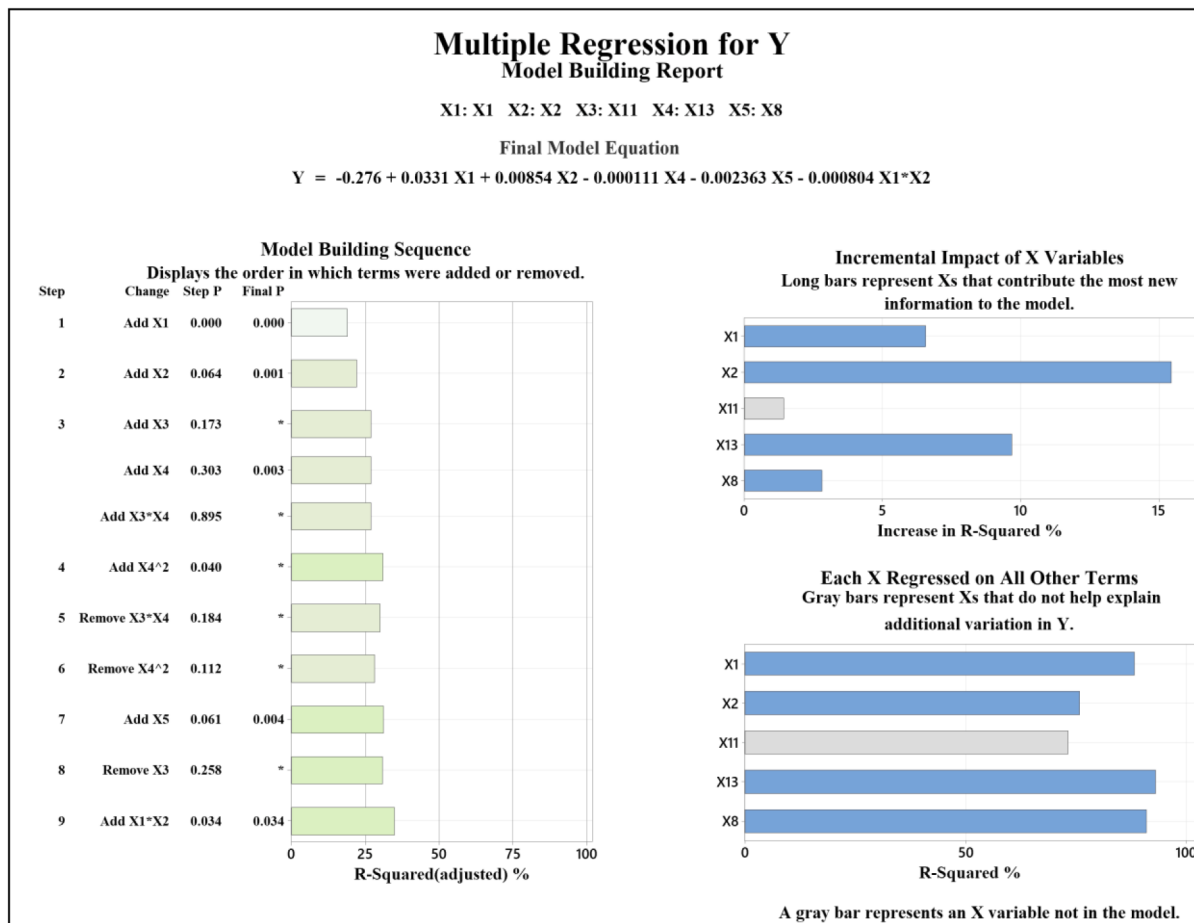


Fig. A1. Minitab 20.3 summary report on the relationship between the variables and yield.



**Fig. A2.** Minitab 20.3 summary report on the variables' contribution to the yield model.

Having established the base value for energy demand and yield, researchers and agricultural practitioners can conduct resource efficiency to identify areas with less energy consumption or suboptimal yields, prompting targeted interventions for improvement. Comparative analysis of different greenhouse designs (such as PCM type, orientation, location, among others), technologies, and management practices can also be conducted to identify which parameters significantly affect energy consumption and yield, leading to insights about the most effective ways to optimize these aspects. On sustainability, by researching and implementing strategies to reduce energy consumption in greenhouse environments, the overall ecological footprint of agriculture can be lowered, making the industry more sustainable in the long run. By identifying design parameters that result in energy savings without compromising crop yield and quality, farmers can enhance their profitability. Food security and regulatory compliance are other reasons this study is of importance.

In summary, establishing a baseline for energy demand and yield in greenhouse environments provides a solid starting point for conducting research to optimize energy consumption and promote sustainable and efficient agricultural practices. Researchers can uncover innovative solutions that balance productivity, resource efficiency, and environmental responsibility by exploring various greenhouse design parameters.

#### 4. Conclusion

In conclusion, this comprehensive study has successfully established fundamental parameters for a single-span double-layer with a thermal

screen (DVBES) greenhouse, shedding light on energy demand and strawberry yield considerations. Through the innovative development of a ventilated DVBES model within the TRNSYS 18 software, the research not only accurately predicts critical greenhouse parameters such as energy consumption, temperature, and relative humidity but also introduces a strawberry yield model that incorporates essential factors like temperature, relative humidity, and solar radiation. The precision of this yield model, showcasing minimal errors, underscores its reliability.

The study's findings provide valuable insights for greenhouse management and sustainable agricultural practices. For a specific scenario represented by the Daegu location with an east–west ( $90^\circ$ ) orientation, the established base case parameters indicate an energy demand of  $113.861 \text{ MJ.m}^{-2}$  and a corresponding strawberry yield of  $0.466 \text{ kg. plant}^{-1}$  over a winter season. These outcomes contribute to optimizing greenhouse operations, facilitating informed decision-making for energy consumption and crop productivity.

Overall, the integration of advanced modeling techniques and empirical data not only advances our understanding of greenhouse dynamics but also offers a framework for future research endeavors to enhance resource efficiency, crop yield, and environmental sustainability within controlled agricultural environments.

#### Declaration of Competing Interest

The authors declare that they have no known competing financial interests or personal relationships that could have appeared to influence the work reported in this paper.

## Acknowledgements

This work acknowledged the effort of Mr. Muhammed Taofiq Hamza; Adelodun, Bashir (PhD.) and Ahmad, M. Junaid (PhD).

## Funding

This work was supported by the Korea Institute of Planning and Evaluation for Technology in Food, Agriculture, Forestry (IPET) through Agriculture, Food and Rural Affairs Convergence Technologies Program for Educating Creative Global Leader, funded by Ministry of Agriculture, Food and Rural Affairs (MAFRA) (717001-7). This research was supported by Basic Science Research Program through the National Research Foundation of Korea (NRF), funded by the Ministry of Education [NRF-2019R1I1A3A01051739].

## Appendix

**Fig. A1**  
**Fig. A2**

## References

- [1] T.D. Akpenpuun, et al., Building Energy Simulation model application to greenhouse microclimate, covering material and thermal blanket modelling: A Review, *Niger. J. Technol. Dev.* 19 (3) (2022) 3851–3856.
- [2] D. Mazzeo, N. Matera, C. Cornaro, G. Oliveti, P. Romagnoni, L. De Santoli, EnergyPlus, IDA ICE and TRNSYS predictive simulation accuracy for building thermal behaviour evaluation by using an experimental campaign in solar test boxes with and without a PCM module, *Energy Build.* 212 (2020) 109812.
- [3] A. Rasheed, C.S. Kwak, W.H. Na, J.W. Lee, H.T. Kim, H.W. Lee, Development of a Building Energy Simulation Model for Control of Multi-Span Greenhouse Microclimate, *Agronomy* 10 (9) (2020) pp, <https://doi.org/10.3390/agronomy10091236>.
- [4] T. Boulard, H. Fatnassi, H. Majdoubi, L. Bouirden, Airflow and microclimate patterns in a one-hectare canary type greenhouse: An experimental and CFD assisted study, *Acta Hortic.* vol. 801 PART 2(6) (2008) 837–845, <https://doi.org/10.17660/actahortic.2008.801.98>.
- [5] O. As'a'd, V.I. Ugursal, N. Ben-Abdallah, "Investigation of the energetic performance of an attached solar greenhouse through monitoring and simulation", *Energy Sustain. Dev.* 53 (2019) 15–29.
- [6] N. Choab, A. Allouhi, A. El Maakoul, T. Kousksou, S. Saadeddine, A. Jamil, Effect of Greenhouse Design Parameters on the Heating and Cooling Requirement of Greenhouses in Moroccan Climatic Conditions, *IEEE Access* 9 (2021) 2986–3003, <https://doi.org/10.1109/ACCESS.2020.3047851>.
- [7] A. Rasheed, J.W. Lee, H.W. Lee, Development and optimization of a building energy simulation model to study the effect of greenhouse design parameters, *Energies* 11 (8) (2018) pp, <https://doi.org/10.3390/en11082001>.
- [8] A. Rasheed, W.H. Na, J.W. Lee, H.T. Kim, H.W. Lee, Optimization of greenhouse thermal screens for maximized energy conservation, *Energies* 12 (19) (2019) 1–20, <https://doi.org/10.3390/en12193592>.
- [9] R. Ward, R. Choudhary, C. Cundy, G. Johnson, and A. Mcrobie, "Simulation of plants in buildings; incorporating plant-Air interactions in building energy simulation," *14th Int. Conf. IBPSA - Build. Simul. 2015, BS 2015, Conf. Proc.*, pp. 2256–2263, 2015.
- [10] A. Rabiu, W.-H. Na, T.D. Akpenpuun, A. Rasheed, M.A. Adesanya, Q.O. Ogunlowo, H.T. Kim, H.-W. Lee, Determination of overall heat transfer coefficient for greenhouse energy-saving screen using Trnsys and hotbox, *Biosyst. Eng.* 217 (2022) 83–101.
- [11] M.A. Adesanya W.-H. Na A. Rabiu Q.O. Ogunlowo T.D. Akpenpuun A. Rasheed Y.-C. Yoon H.-W. Lee TRNSYS Simulation and Experimental Validation of Internal Temperature and Heating Demand in a Glass Greenhouse Sustainability 14 14 8283.
- [12] T.Q.Z. Cesar, P.A.M. Leal, O.C. Branquinho, F.A.M. Miranda, Wireless sensor network to identify the reduction of meteorological gradients in greenhouse in subtropical conditions, *J. Agric. Eng.* 52 (1) (2021) 1–8, <https://doi.org/10.4081/jae.2020.1105>.
- [13] M.A. Lamrani, T. Boulard, J.C. Roy, A. Jaffrin, Airflows and temperature patterns induced in a confined greenhouse, *J. Agric. Eng. Res.* 78 (1) (2001) 75–88, <https://doi.org/10.1006/jaer.2000.0568>.
- [14] M. Zhao, Y. Teitel, M; Barak, "Vertical temperature and humidity gradients in a naturally ventilated greenhouse", *J. Agric. Eng. Res.* 78 (4) (2001) 431–436.
- [15] Q.O. Ogunlowo T.D. Akpenpuun W.-H. Na A. Rabiu M.A. Adesanya K.S. Addae H.-T. Kim H.-W. Lee Analysis of Heat and Mass Distribution in a Single- and Multi-Span Greenhouse Microclimate Agriculture 11 9 891.
- [16] C. Baglivo, D. Mazzeo, S. Panico, S. Bonuso, N. Matera, P.M. Congedo, G. Oliveti, Complete greenhouse dynamic simulation tool to assess the crop thermal well-being and energy needs, *Appl. Therm. Eng.* 179 (2020) 115698.
- [17] R. Gupta, "An Introduction to Discretization Techniques for Data Scientistse", *Towards Data*, accessed May 30, 2022, Science (2019), <https://towardsdatascience.com/an-introduction-to-discretization-in-data-science-55ef8c9775a2>.
- [18] TRANSSOLAR Energietechnik, Multizone Building modeling with Type56 and TRNBuild [Online]. Available: Trnsys 18, 5 (2017) 49–50 <http://www.trnsys.com/>.
- [19] Q.O. Ogunlowo, et al., Effect of envelope characteristics on the accuracy of discretised greenhouse model in TRNSYS, *J Agric. Eng. vol. LIII*, no. 1420 (2022), <https://doi.org/10.4081/jae.2022.1420>.
- [20] N. Laghmich, Z. Romani, R. Lapisa, A. Draoui, Numerical analysis of horizontal temperature distribution in large buildings by thermo-aeraulic zonal approach, *Build. Simul.* 15 (1) (2022) 99–115.
- [21] Y. Shen, R. Wei, L. Xu, Energy consumption prediction of a greenhouse and optimization of daily average temperature, *Energies* 11 (1) (2018) pp, <https://doi.org/10.3390/en11010065>.
- [22] A. Jayalath, L. Aye, P. Mendis, T. Ngo, Effects of phase change material roof layers on thermal performance of a residential building in Melbourne and Sydney, *Energy Build.* 121 (2016) 152–158, <https://doi.org/10.1016/j.enbuild.2016.04.007>.
- [23] L. Boussaba, G. Lefebvre, Investigation of White Vaseline as an alternative phase change material for thermal regulation of physiological birth rooms, *Journal of Building Engineering* 44 (2021) 102669.
- [24] M. Zhao School of Energy and Power Engineering, Inner Mongolia University of Technology, Hohhot 010051, China Y. Liu School of Energy and Power Engineering, Inner Mongolia University of Technology, Hohhot 010051, China D. Bao School of Energy and Power Engineering, Inner Mongolia University of Technology, Hohhot 010051, China X. Hu School of Energy and Power Engineering, Inner Mongolia University of Technology, Hohhot 010051, China N. Wang School of Energy and Power Engineering, Inner Mongolia University of Technology, Hohhot 010051, China L. Liu School of Energy and Power Engineering, Inner Mongolia University of Technology, Hohhot 010051, China Study on the Influence of Solar Array Tube on Thermal Environment of Greenhouse Sustain. 15 4 2023 10.3390/su15043127 3127.
- [25] Z. Naghibi, D.S. Ting, Improving clean energy greenhouse heating with solar thermal energy storage and phase change materials, *Energy Storage* vol. e116, no. November (2019) 1–14, <https://doi.org/10.1002/est2.116>.
- [26] A. Najjar, A. Hasan, Modeling of greenhouse with PCM energy storage, *Energy Convers. Manag.* 49 (2008) (2008) 3338–3342, <https://doi.org/10.1016/j.enconman.2008.04.015>.
- [27] C. Cornaro, M. Pierro, V.A. Puggioni, D. Roncarati, Outdoor Characterization of Phase Change Materials Reach NZEB, *Buildings* 7 (55) (2017) 1–19, <https://doi.org/10.3390/buildings7030055>.
- [28] G.P. Panayiotou, S.A. Kalogirou, S.A. Tassou, Evaluation of the application of Phase Change Materials (PCM) on the envelope of a typical dwelling in the Mediterranean region, *Renew. Energy* 97 (2016) 24–32, <https://doi.org/10.1016/j.renene.2016.05.043>.
- [29] J. Virgone, K. Johannes, F. Kuznik, Development and validation of a new TRNSYS type for the simulation of external building walls containing PCM, *Energy Build.* 42 (7) (2010) 1004–1009, <https://doi.org/10.1016/j.enbuild.2010.01.012>.
- [30] H. Schranzhofer, P. Puschning, A. Heinz, and W. Streicher, "Validation of a TRNSYS Simulation Model for PCM Energy Storages and PCM Wall Construction Elements," in *10th International Conference on Thermal Energy Storage*, 2006, pp. 2–7.
- [31] M. E. Poulad, A. S. Fung, and D. Naylor, "Effects of Convective Heat Transfer Coefficient on the Ability of PCM to Reduce Building Energy Demand," in *12th Conference of International Building Performance Simulation Association*, 2011, pp. 270–277.
- [32] Q.O. Ogunlowo, et al., Development of a 'PCM in Container' Energy Storage Model Component for a Possible Building Energy Evaluation in TRNSYS 18, *Biosyst. Eng.* (2023).
- [33] H.S. Sim, D.S. Kim, M.G. Ahn, S.R. Ahn, S.K. Kim, Prediction of strawberry growth and fruit yield based on environmental and growth data in a greenhouse for soil cultivation with applied autonomous facilities, *Hortic. Sci. Technol.* 38 (6) (2020) 840–849, <https://doi.org/10.7235/HORT.202000076>.
- [34] E. Mashonjowa, F. Ronsse, J.R. Milford, J.G. Pieters, Modelling the thermal performance of a naturally ventilated greenhouse in Zimbabwe using a dynamic greenhouse climate model, *Sol. Energy* 91 (2013) 381–393.
- [35] Y. Ishigami, E. Goto, M. Watanabe, T. Takahashi, L. Okushima, DEVELOPMENT OF A SIMULATION MODEL TO EVALUATE ENVIRONMENTAL CONTROLS IN A TOMATO GREENHOUSE, *Acta Hortic.* 1037 (2014) 93–98, <https://doi.org/10.17660/ActaHortic.2014.1037.7>.
- [36] B. Khoshnevisan, S. Rafiee, H. Mousazadeh, Environmental impact assessment of open field and greenhouse strawberry production, *Eur. J. Agron.* 50 (2013) 29–37, <https://doi.org/10.1016/j.eja.2013.05.003>.
- [37] Y. Tang, X. Ma, M. Li, Y. Wang, The effect of temperature and light on strawberry production in a solar greenhouse, *Solar Energy* 195 (2020) 318–328.

- [38] A. Sønsteby, K.A. Solhaug, O.M. Heide, Functional growth analysis of 'Sonata' strawberry plants grown under controlled temperature and daylength conditions, *Sci. Hortic.* (amsterdam) 211 (2016) 26–33, <https://doi.org/10.1016/j.scientia.2016.08.003>.
- [39] ASHRAE, *2021 ASHRAE® Handbook. Fundamentals*. 2021.
- [40] ASHRAE Technical Committee, *ASHRAE Handbook: Heating, Ventilating and Air-Conditioning Applications Inch-Pound Edition*. 2015.
- [41] W.C. Lin, CROP MODELLING AND YIELD PREDICTION FOR GREENHOUSE-GROWN LETTUCE, *Acta Hortic.* 593 (2002) 159–164, <https://doi.org/10.17660/ActaHortic.2002.593.20>.
- [42] G. Odey, B. Adelodun, G. Cho, S. Lee, K.A. Adeyemi, K.S. Choi, Modeling the Influence of Seasonal Climate Variability on Soybean Yield in a Temperate Environment: South Korea as a Case Study, *Int. J. Plant Prod.* 16 (2) (2022) 209–222, <https://doi.org/10.1007/s42106-022-00188-2>.
- [43] G. Casella, *Statistical inference*, Second, Duxbury/Thompson Learning, Pacific Grove, California, 2002.
- [44] The Engineering ToolBox, Fossil and Alternative Fuels - Energy Content, accessed Apr. 03, 2023, Online (2008), [https://www.engineeringtoolbox.com/fossil-fuels-energy-content-d\\_1298.html](https://www.engineeringtoolbox.com/fossil-fuels-energy-content-d_1298.html).